

# Nonequilibrium Spin-Glass Dynamics from Picoseconds to a Tenth of a Second

F. Belletti,<sup>1</sup> M. Cotallo,<sup>2</sup> A. Cruz,<sup>3,2</sup> L. A. Fernandez,<sup>4,2</sup> A. Gordillo-Guerrero,<sup>5,2</sup> M. Guidetti,<sup>1</sup> A. Maiorano,<sup>1,2</sup> F. Mantovani,<sup>1</sup> E. Marinari,<sup>6</sup> V. Martin-Mayor,<sup>4,2</sup> A. Muñoz Sudupe,<sup>4</sup> D. Navarro,<sup>7</sup> G. Parisi,<sup>6</sup> S. Perez-Gaviro,<sup>2</sup> J. J. Ruiz-Lorenzo,<sup>5,2</sup> S. F. Schifano,<sup>1</sup> D. Sciretti,<sup>2</sup> A. Tarancon,<sup>3,2</sup> R. Tripicciono,<sup>1</sup> J. L. Velasco,<sup>2</sup> and D. Yllanes<sup>4,2</sup>

<sup>1</sup>*Dipartimento di Fisica Università di Ferrara and INFN - Sezione di Ferrara, Ferrara, Italy*

<sup>2</sup>*Instituto de Biocomputación y Física de Sistemas Complejos (BIFI), Zaragoza, Spain*

<sup>3</sup>*Departamento de Física Teórica, Universidad de Zaragoza, 50009 Zaragoza, Spain*

<sup>4</sup>*Departamento de Física Teórica I, Universidad Complutense, 28040 Madrid, Spain*

<sup>5</sup>*Departamento de Física, Universidad de Extremadura, 06071 Badajoz, Spain*

<sup>6</sup>*Dipartimento di Fisica, INFN and INFN, Università di Roma "La Sapienza", 00185 Roma, Italy*

<sup>7</sup>*D. de Ingeniería, Electrónica y Comunicaciones and I3A, U. de Zaragoza, 50018 Zaragoza, Spain*

(Received 11 April 2008; revised manuscript received 23 June 2008; published 6 October 2008)

We study numerically the nonequilibrium dynamics of the Ising spin glass, for a time spanning 11 orders of magnitude, thus approaching the experimentally relevant scale (i.e., *seconds*). We introduce novel analysis techniques to compute the coherence length in a model-independent way. We present strong evidence for a replicon correlator and for overlap equivalence. The emerging picture is compatible with noncoarsening behavior.

DOI: 10.1103/PhysRevLett.101.157201

PACS numbers: 75.10.Nr, 75.40.Gb, 75.40.Mg, 75.50.Lk

Spin glasses [1] (SG) exhibit remarkable features, including slow dynamics and a complex space of states: they are a paradigmatic problem because of its many applications to glassy behavior, optimization, biology, financial markets, social dynamics, etc.

Experiments on SG [1,2] focus on nonequilibrium dynamics. In the simplest protocol, isothermal aging, the SG is cooled as fast as possible to a subcritical working temperature,  $T < T_c$ , let to equilibrate for a *waiting time*,  $t_w$ , and probed at a later time,  $t + t_w$ . The thermoremanent magnetization is found to be a function of  $t/t_w$  (*full aging*), for  $10^{-3} < t/t_w < 10$  and  $50 \text{ s} < t_w < 10^4 \text{ s}$  [3] (see, however, [4]). The growing size of the coherent domains, the coherence-length  $\xi$ , is also measured [5,6]. Two features emerge: (i) the lower  $T$ , the slower the growth of  $\xi(t_w)$  and (ii)  $\xi \sim 100$  lattice spacings, even for  $T \sim T_c$  and  $t_w \sim 10^4 \text{ s}$  [5].

The sluggish dynamics arises from a thermodynamic transition at  $T_c$  [7–9]. There is a sustained theoretical debate on the properties of the (unreachable in human times) equilibrium low  $T$  SG phase, which is nevertheless relevant to (basically nonequilibrium) experiments [10]. The main scenarios are the droplets [11], replica symmetry breaking (RSB) [12], and the intermediate trivial-nontrivial (TNT) picture [13].

Droplets expects two equilibrium states related by global spin reversal. The SG order parameter, the spin overlap  $q$ , takes only two values  $q = \pm q_{EA}$ . In the RSB scenario an infinite number of pure states influence the dynamics [12,14,15], so all  $-q_{EA} \leq q \leq q_{EA}$  are reachable. In TNT the SG phase is similar to an antiferromagnet with random boundary conditions:  $q$  behaves as for RSB systems but, similar to droplets, the surface-to-volume ratio of the largest thermally activated domains

vanishes (i.e., the link-overlap defined below takes a single value).

Because of superuniversality [16], the isothermal aging of basically all coarsening systems is qualitatively the same (droplets being analogous to a disguised ferromagnet [17]). For  $T < T_c$  the dynamics consists in the growth of compact domains, where the spin overlap takes one of the values  $q = \pm q_{EA}$ . The corresponding growth law,  $\xi(t)$ , completely encodes all time dependencies. The antiferromagnet analogy suggests a similar TNT aging.

Since in the RSB scenario  $q = 0$  equilibrium states do exist, the nonequilibrium dynamics starts with a vanishing order parameter and remains there forever. The replicon, a critical mode analogous to magnons in Heisenberg ferromagnets, is present for all  $T < T_c$  [18]. Furthermore,  $q$  is not a privileged observable (overlap equivalence [14]): the link overlap displays equivalent aging behavior.

These theories need numerics to be quantitative [19–27]. Simulations so far have been too short: experimental scales are at  $\sim 100 \text{ s}$ , while typical nonequilibrium simulations reach  $\sim 10^{-5} \text{ s}$  (one Monte Carlo step, MCS, corresponds to  $10^{-12} \text{ s}$  [1]). Over the years, high-performance computers have been built for SG simulations [28–30].

Here we report on a large simulation ( $10^{11}$  MCS  $\sim 0.1 \text{ s}$ ) of an instantaneous SG quench protocol performed on the Janus computer [30], which allows us to reach experimental times by mild extrapolations. Aging is investigated as a function of time and temperature. We obtain model-independent determinations of the SG coherence length  $\xi$ . Conclusive evidence is presented for a critical correlator associated with the replicon mode. We observe nontrivial aging in the link correlation (a *nonequilibrium* test of overlap equivalence [14]). We conclude that, up to experimental scales, SG dynamics is not coarsening like.

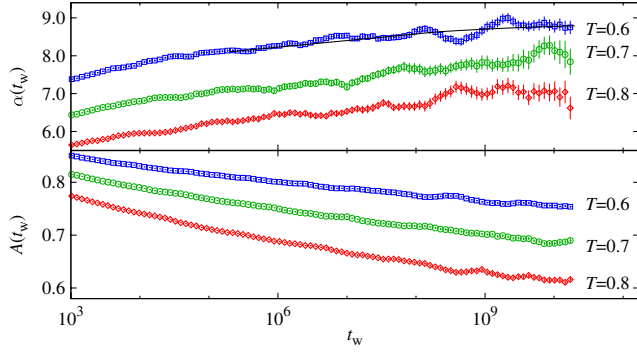


FIG. 1 (color online). Fit parameters,  $A$  and  $\alpha$  ( $C(t, t_w) = A(t_w)(1 + t/t_w)^{-1/\alpha(t_w)}$ ) vs  $t_w$  for temperatures below  $T_c$  ( $T = 0.6$  line: fit, for  $t_w > 10^5$ , to  $\alpha(t_w) = \alpha_0 + \alpha_1 \log t_w + \alpha_2 \log^2 t_w$ ,  $\alpha_0 = 6.35795$ ,  $\alpha_1 = 0.18605$ ,  $\alpha_2 = -0.00351835$ , diagonal  $\chi^2/\text{d.o.f.} = 66.26/63$ ). Oscillations are due to strong correlations of  $\alpha(t_w)$  at neighboring times (the fit and  $\chi^2/\text{d.o.f.}$  do not change if we bin data in blocks of 5 consecutive  $t_w$ ).

The  $D = 3$  Edwards-Anderson Hamiltonian is

$$\mathcal{H} = - \sum_{\langle x, y \rangle} J_{x, y} \sigma_x \sigma_y, \quad (1)$$

( $\langle \cdots \rangle$  denote nearest neighbors). Spins  $\sigma_x = \pm 1$  sit at the nodes,  $x$ , of a cubic lattice of size  $L$  and periodic boundary conditions. The couplings (quenched variables)  $J_{x, y} = \pm 1$  are chosen randomly with 50% probability. For each set of couplings (a sample), we simulate two independent systems,  $\{\sigma_x^{(1)}\}$  and  $\{\sigma_x^{(2)}\}$ . We denote by  $\overline{(\cdots)}$  the average over the couplings. Model (1) has a SG transition at  $T_c = 1.101(5)$  [31].

Our  $L = 80$  systems evolve with Heat-Bath dynamics [32], which is in the Universality Class of physical evolution. Fully disordered starting spin configurations are placed at the working temperature (96 samples at  $T = 0.8 \approx 0.73T_c$  and at  $T = 0.6 \approx 0.54T_c$ ; 64 at  $T = 0.7 \approx 0.64T_c$ ). We also perform shorter simulations (32 samples) at  $T_c$ , and  $L = 40$  and  $L = 24$  runs to check for finite-size effects.

A crucial quantity is the two-times correlation function [19,20,23]: [ $c_x(t, t_w) \equiv \sigma_x(t + t_w)\sigma_x(t_w)$ ]

$$C(t, t_w) = L^{-3} \sum_x \overline{c_x(t, t_w)}, \quad (2)$$

linearly related to the real part of the a.c. susceptibility at waiting time  $t_w$  and frequency  $\omega = \pi/t$ .

To check for full aging [3] in a systematic way, we fit  $C(t, t_w)$  as  $A(t_w)(1 + t/t_w)^{-1/\alpha(t_w)}$  in the range  $t_w \leq t \leq 10t_w$  [33], obtaining fair fits for all  $t_w > 10^3$ ; see Fig. 1. To be consistent with the experimental claim of full-aging behavior for  $10^{14} < t_w < 10^{16}$  [3],  $\alpha(t_w)$  should be constant in this  $t_w$  range. Although  $\alpha(t_w)$  keeps growing for our largest times (with the large errors in [23] it seemed

constant for  $t_w > 10^4$ ), its growth slows down. The behavior at  $t_w = 10^{16}$  seems beyond reasonable extrapolation.

The coherence length is studied from the correlations of the replica field  $q_x(t_w) \equiv \sigma_x^{(1)}(t_w)\sigma_x^{(2)}(t_w)$ ,

$$C_4(r, t_w) = L^{-3} \sum_x \overline{q_x(t_w)q_{x+r}(t_w)}. \quad (3)$$

For  $T < T_c$ , it is well described by [12,21]

$$C_4(r, t_w) \sim r^{-a} e^{-(r/\xi(t_w))^b}, \quad a \simeq 0.5, \quad b \simeq 1.5. \quad (4)$$

The actual value of  $a$  is relevant. For coarsening dynamics  $a = 0$ , while in a RSB scenario  $a > 0$  and  $C_4(r, t_w)$  vanishes at long times for fixed  $r/\xi(t_w)$ . At  $T_c$ , the latest estimate is  $a = 1 + \eta = 0.616(9)$  [31].

To study  $a$  independently of a particular Ansatz as (4) we consider the integrals

$$I_k(t_w) = \int_0^\infty dr r^k C_4(r, t_w), \quad (5)$$

(e.g., the SG susceptibility is  $\chi^{\text{SG}}(t_w) = 4\pi I_2(t_w)$ ). As we assume  $L \gg \xi(t_w)$  we safely reduce the upper limit to  $L/2$ . If a scaling form  $C_4(r, t_w) \sim r^{-a} f[r/\xi(t_w)]$  is adequate at large  $r$ , then  $I_k(t_w) \propto [\xi(t_w)]^{k+1-a}$ . It follows that  $\xi_{k,k+1}(t_w) \equiv I_{k+1}(t_w)/I_k(t_w)$  is proportional to  $\xi(t_w)$  and  $I_1(t_w) \propto \xi_{1,2}^{2-a}$ . We find  $\xi^{(2)}(t_w) \approx 0.8\xi_{1,2}(t_w)$ , where  $\xi^{(2)}$  is the noisy second-moment estimate [9]. Furthermore, for  $\xi_{1,2} > 3$ , we find  $\xi_{0,1}(t_w) \approx 0.46\xi_{1,2}(t_w)$ , and  $\xi^{\text{fit}}(t_w) = 1.06\xi_{1,2}(t_w)$ , ( $\xi^{\text{fit}}$  from a fit to (4) with  $a = 0.4$ ).

Note that, when  $\xi \ll L$ , irrelevant distances  $r \gg \xi$  largely increase statistical errors for  $I_k$ . Fortunately, the very same problem was encountered in the analysis of correlated time series [34], and we may borrow the cure [35].

The largest  $t_w$  where  $L = 80$  still represents  $L = \infty$  physics follows from finite-size scaling [32]: for a given

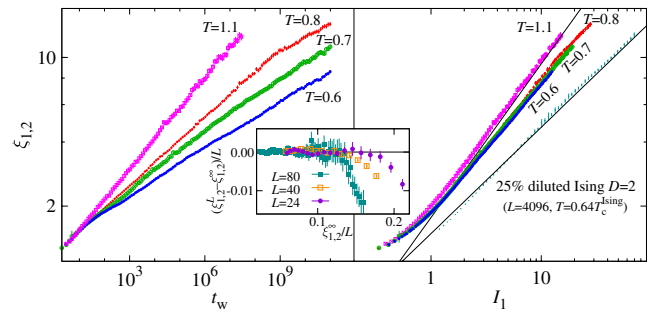


FIG. 2 (color online). Left: SG coherence length  $\xi_{1,2}$  vs waiting time, for  $T \leq T_c$ . Right:  $\xi_{1,2}$  vs  $I_1$ , ( $\xi_{1,2} \propto I_1^{1/(2-a)}$ ). Also shown data for the site-diluted Ising model ( $\xi_{1,2}$  and  $I_1$  rescaled by 2). Full lines: Ising (coarsening,  $a = 0$ ) and SG,  $a(T_c) = 0.616$  [31]. Inset:  $[\xi_{1,2}(t_w) - \xi_{1,2}^\infty(t_w)]/L$  vs  $\xi_{1,2}^\infty(t_w)/L$  for  $T = 0.8$  and  $L = 24, 40$  and  $80$  ( $\xi_{1,2}^\infty(t_w)$  from a fit  $\xi_{1,2}(t_w) = A(T)t_w^{1/z(T)}$  for  $L = 80$  in the range  $3 < \xi_{1,2} < 10$ ).

numerical accuracy, one should have  $L \geq k\xi_{1,2}(t_w)$ . To compute  $k$ , we compare  $\xi_{1,2}^L$  for  $L = 24, 40$  and  $80$  with  $\xi_{1,2}^\infty$  estimated with the power law described below (Fig. 2, inset). It is clear that the safe range is  $L \geq 7\xi_{1,2}(t_w)$  at  $T = 0.8$  (at  $T_c$  the safety bound is  $L \geq 6\xi_{1,2}(t_w)$ ).

Our results for  $\xi_{1,2}$  are shown in Fig. 2. Note for  $T = 0.8$  the finite-size change of regime at  $t_w = 10^9$  ( $\xi_{1,2} \sim 11$ ). We find fair fits to  $\xi(t_w) = A(T)t_w^{1/z(T)}$ :  $z(T_c) = 6.86(16)$ ,  $z(0.8) = 9.42(15)$ ,  $z(0.7) = 11.8(2)$  and  $z(0.6) = 14.1(3)$ , in good agreement with previous numerical and experimental findings  $z(T) = z(T_c)T_c/T$  [5,21]. Our fits are for  $3 \leq \xi \leq 10$ , to avoid both finite-size and lattice discretization effects. Extrapolating to experimental times ( $t_w = 10^{14} \sim 100$  s), we find  $\xi = 14.0(3)$ ,  $21.2(6)$ ,  $37.0(14)$ , and  $119(9)$  for  $T = 0.6$ ,  $T = 0.7$ ,  $T = 0.8$  and  $T = 1.1 \approx T_c$ , respectively, which nicely compares with experiments [5,6].

In Fig. 2, we also explore the scaling of  $I_1$  as a function of  $\xi_{1,2}$  ( $I_1 \propto \xi^{2-a}$ ). The nonequilibrium data for  $T = 1.1$  scales with  $a = 0.585(12)$ . The deviation from the *equilibrium* estimate  $a = 0.616(9)$  [31] is at the limit of statistical significance (if present, it would be due to scaling corrections). For  $T = 0.8, 0.7$ , and  $0.6$ , we find  $a = 0.442(11)$ ,  $0.355(15)$ , and  $0.359(13)$ , respectively (the residual  $T$  dependence is probably due to critical effects still felt at  $T = 0.8$ ). Note that ground state computations for  $L \leq 14$  yielded  $a(T = 0) \approx 0.4$  [37]. These numbers differ both from critical and coarsening dynamics ( $a = 0$ ).

We finally address the aging properties of  $C_{\text{link}}(t, t_w)$

$$C_{\text{link}}(t, t_w) = \frac{\sum_{\langle x, y \rangle} c_x(t, t_w) c_y(t, t_w)}{(3L^3)}. \quad (6)$$

$C_{\text{link}}$ , still experimentally inaccessible, does not vanish if the configurations at  $t + t_w$  and  $t_w$  differ by the spin inversion of a compact region of half the system size.

It is illuminating to replace  $t$  with  $C^2(t, t_w)$  as an independent variable; Figs. 3 and 4. For a coarsening dynamics  $C_{\text{link}}$  will be  $C$  independent for  $C^2 < q_{\text{EA}}^2$  and large  $t_w$  (relevant system excitations are the spin reversal of compact droplets not affecting  $C_{\text{link}}$ ), while in a RSB system

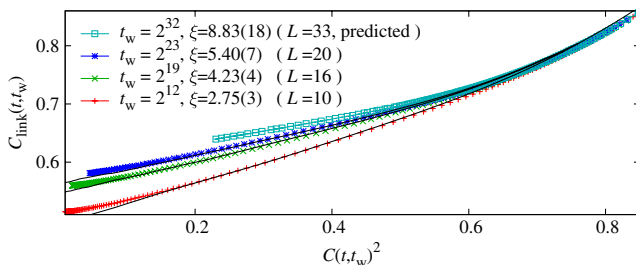


FIG. 3 (color online). For appropriate  $t_w$  and  $L$ , the nonequilibrium  $C_{\text{link}}(t, t_w)$  vs  $C^2(t, t_w)$  at  $T = 0.7$ , coincides with equilibrium  $Q_{\text{link}}|_q$  vs  $q^2$  (full lines, equilibrium data from [40] at  $T = 0.7$ , see text). From the length-time dictionary up to  $L = 20$  we predict the equilibrium curve for  $L = 33$ .

new states are continuously found as time goes by: we expect a non constant  $C^2$  dependence even if  $C < q_{\text{EA}}$  [38].

By general arguments, the nonequilibrium  $C_{\text{link}}$  at finite times coincides with equilibrium correlation functions for systems of finite size [10]; see Fig. 3. We also predict the  $q^2$  dependency of the *equilibrium* conditional expectation  $Q_{\text{link}}|_q$  up to  $L = 33$  [ $Q_{\text{link}}$  is just  $C_4(r = 1)$ , while  $q$  is the spatial average of  $q_x$ , Eq. (3)].

As for the shape of the curve  $C_{\text{link}} = f(C^2, t_w)$ , Fig. 4 bottom, the  $t_w$  dependency is residual. Within our time window,  $C_{\text{link}}$  is not constant for  $C < q_{\text{EA}}$ . For comparison (inset) we show the qualitatively different curves for a coarsening dynamics. We studied the derivative  $dC_{\text{link}}/dC^2$ , for  $C^2 < q_{\text{EA}}^2$ , Fig. 4 top. We first smooth the curves by fitting  $C_{\text{link}} = f(C^2)$  to the lowest order polynomial allowing a fair fit (seventh order for  $t_w \leq 2^{25}$ , sixth for larger  $t_w$ ), whose derivative was taken afterwards (jack-knife statistical errors).

Furthermore, we have extrapolated both  $C_{\text{link}}(t = rt_w, t_w)$  and  $C(t = rt_w, t_w)$  to  $t_w \approx 10^{14}$  ( $\sim 100$  s), for  $r = 8, 4, \dots, \frac{1}{16}$  [39]. The extrapolated points for  $t_w = 10^{14}$  fall on a straight line whose slope is plotted in the upper panel (thick line). The derivative is nonvanishing for  $C^2 < q_{\text{EA}}^2$ , for the experimental time scale.

In summary, Janus [30] halves the (logarithmic) time gap between simulations and nonequilibrium spin-glass experiments. We analyzed the simplest temperature quench, finding numerical evidence for a noncoarsening dynamics, at least up to experimental times (see also [27]). Let us highlight: *nonequilibrium* overlap equivalence (Figs. 3 and 4); nonequilibrium scaling functions reproducing *equilibrium* conditional expectations in finite systems

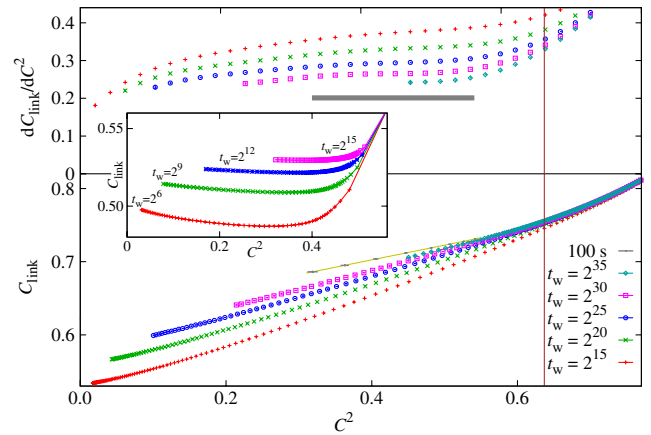


FIG. 4 (color online). Bottom:  $C_{\text{link}}(t, t_w)$  vs  $C^2(t, t_w)$  for  $T = 0.6$  and some of our largest  $t_w$  (vertical line:  $q_{\text{EA}}^2$  from [24]). We also show our extrapolation of the  $C_{\text{link}}$  vs  $C^2$  curve to  $t_w = 10^{14}$  ( $\sim 100$  s, see text). Top: Derivative of  $C_{\text{link}}$  with respect to  $C^2$  for  $T = 0.6$ . The horizontal line corresponds to the slope of a linear fit of  $t_w = 10^{14}$  extrapolations (the line width equals twice the error). Inset: As in bottom panel, for the ferromagnetic site-diluted  $D = 2$  Ising model (same simulation of Fig. 2).

(Fig. 3); and a nonequilibrium replicon exponent compatible with equilibrium computations [37]. The growth of the coherence length sensibly extrapolates to  $t_w = 100$  s (our analysis of dynamic heterogeneities [26,27] will appear elsewhere [36]). Exploring with Janus nonequilibrium dynamics up to the *seconds* scale will allow the investigation of many intriguing experiments.

We corresponded with M. Hasenbusch, A. Pelissetto, and E. Vicari. Janus was supported by EU FEDER funds (UNZA05-33-003, MEC-DGA, Spain), and developed in collaboration with ETHlab. We were partially supported by MEC (Spain), through Contracts No. FIS2006-08533, FIS2007-60977, FPA2004-02602, TEC2007-64188; by CAM (Spain), and by Microsoft.

- 
- [1] J. A. Mydosh, *Spin Glasses: an Experimental Introduction* (Taylor and Francis, London, 1993).
  - [2] E. Vincent *et al.*, in *Lecture Notes in Physics*, edited by M. Rubí and C. Pérez-Vicente (Springer, New York, 1997), Vol. 492.
  - [3] G. F. Rodriguez, G. G. Kenning, and R. Orbach, Phys. Rev. Lett. **91**, 037203 (2003).
  - [4] V. Dupuis *et al.*, Pramana J. Phys. **64**, 1109 (2005).
  - [5] Y. G. Joh *et al.*, Phys. Rev. Lett. **82**, 438 (1999).
  - [6] F. Bert *et al.*, Phys. Rev. Lett. **92**, 167203 (2004).
  - [7] K. Gunnarsson *et al.*, Phys. Rev. B **43**, 8199 (1991).
  - [8] M. Palassini and S. Caracciolo, Phys. Rev. Lett. **82**, 5128 (1999).
  - [9] H. G. Ballesteros *et al.*, Phys. Rev. B **62**, 14237 (2000).
  - [10] S. Franz *et al.*, Phys. Rev. Lett. **81**, 1758 (1998); J. Stat. Phys. **97**, 459 (1999).
  - [11] W. L. McMillan, J. Phys. C **17**, 3179 (1984); A. J. Bray and M. A. Moore, in *Lecture Notes in Physics*, edited by J. L. van Hemmen and I. Morgenstern (Springer, New York, 1987); D. S. Fisher and D. A. Huse, Phys. Rev. Lett. **56**, 1601 (1986); Phys. Rev. B **38**, 386 (1988).
  - [12] E. Marinari *et al.*, J. Stat. Phys. **98**, 973 (2000).
  - [13] F. Krzakala and O. C. Martin, Phys. Rev. Lett. **85**, 3013 (2000); M. Palassini and A. P. Young, Phys. Rev. Lett. **85**, 3017 (2000).
  - [14] G. Parisi and F. Ricci-Tersenghi, J. Phys. A **33**, 113 (2000).
  - [15] P. Contucci and C. Giardinà, J. Stat. Phys. **126**, 917 (2007); Ann. Henri Poincaré **6**, 915 (2005).
  - [16] D. S. Fisher and D. A. Huse, Phys. Rev. B **38**, 373 (1988).
  - [17] Temperature chaos could still spoil the analogy [16].
  - [18] T. Temesvari, C. De Dominicis, and I. Kondor, J. Phys. A **27**, 7569 (1994).
  - [19] J. Kisker *et al.*, Phys. Rev. B **53**, 6418 (1996).
  - [20] H. Rieger, J. Phys. A **26**, L615 (1993).
  - [21] E. Marinari *et al.*, J. Phys. A **33**, 2373 (2000).
  - [22] L. Berthier and J.-P. Bouchaud, Phys. Rev. B **66**, 054404 (2002).
  - [23] S. Jimenez *et al.*, J. Phys. A **36**, 10755 (2003).
  - [24] S. Perez Gavero, J. J. Ruiz-Lorenzo, and A. Tarancón, J. Phys. A **39**, 8567 (2006).
  - [25] S. Jimenez, V. Martin-Mayor, and S. Perez-Gavero, Phys. Rev. B **72**, 054417 (2005).
  - [26] L. C. Jaubert *et al.*, J. Stat. Mech. (2007) P05001; H. E. Castillo *et al.*, Phys. Rev. Lett. **88**, 237201 (2002); H. E. Castillo *et al.*, Phys. Rev. B **68**, 134442 (2003).
  - [27] C. Aron *et al.*, J. Stat. Mech. (2008) P05016.
  - [28] A. Cruz *et al.*, Comput. Phys. Commun. **133**, 165 (2001).
  - [29] A. Ogielski, Phys. Rev. B **32**, 7384 (1985).
  - [30] F. Belletti *et al.*, Comput. Sci. Eng. **8**, 41 (2006); Comput. Phys. Commun. **178**, 208 (2008); arXiv:0710.3535.
  - [31] M. Hasenbusch, A. Pelissetto, and E. Vicari, J. Stat. Mech. L02001 (2008); (private communication).
  - [32] See, e.g., D. J. Amit and V. Martin-Mayor, *Field Theory, the Renormalization Group and Critical Phenomena* (World-Scientific, Singapore, 2005), 3rd ed.
  - [33] Data at different  $t$  and  $t_w$  are correlated, so we consider only diagonal terms in the covariance matrix. Time correlations are considered by first forming jackknife blocks [32] (JKB) with the data for different samples, then minimizing this diagonal  $\chi^2$  for each JKB [23].
  - [34] See, e.g., A. D. Sokal, in *Functional Integration: Basics and Applications* (Cargèse school 1996), edited by C. DeWitt-Morette, P. Cartier, and A. Folacci (Plenum, New Brunswick, 1997).
  - [35] We integrate  $C_4(r, t_w)$  up to  $r^{\text{cutoff}}(t_w)$ , where  $C_4(r^{\text{cutoff}}(t_w), t_w)$  becomes less than thrice its statistical error. We estimate the (small) remaining contribution, by fitting to (4) then integrating the fitted function from  $r^{\text{cutoff}} - 1$  to  $L/2$ . Details will be given elsewhere [36].
  - [36] (Janus Collaboration) (to be published).
  - [37] E. Marinari and G. Parisi, Phys. Rev. Lett. **86**, 3887 (2001).
  - [38]  $C_{\text{link}} = C^2$  in the full-RSB Sherrington-Kirkpatrick model.
  - [39] For each  $r$ , both the link and the spin correlation functions are independently fitted to  $a_r + b_r t_w^{-c_r}$  (fits are stable for  $t_w > 10^5$  with  $c_r \approx 0.5$ ). These fits are then used to extrapolate the two correlation functions to  $t_w = 10^{14}$ .
  - [40] P. Contucci *et al.*, Phys. Rev. Lett. **99**, 057206 (2007); P. Contucci *et al.*, Phys. Rev. Lett. **96**, 217204 (2006).